Application of Simulation-Based Framework to Evaluate Performance of an Optimized Nearly Zero Energy Dwelling During Heatwaves in Belgium

Ramin Rahif[1], Alireza Norouziasas[2], Mohamed Hamdy[2], Shady Attia[1]
[1]Sustainable Building Design Lab, Dept. UEE, Faculty of Applied Sciences, University of Liège, Belgium
[2]Department of Civil and Environmental Engineering, NTNU Norwegian University of Science and Technology, Trondheim, 7491, Norway

Abstract

This study examines three optimal solutions for mitigating overheating caused by disruptions in the cooling system amid heatwaves in Brussels. For this aim, the three highest maximal temperature heatwaves are selected during the 2001-2020, 2040-2060, and 2080-2100 periods based on the Regional Climate Model (MAR) “Modèle Atmosphérique Régional". A multi-indicator approach is applied using operative temperature, heat index, thermal autonomy, and indoor overheating degree metrics. The results reveal that none of the solutions are able to completely prevent overheating, with indoor temperatures reaching more than 29℃. The findings offer a distinct overview of climate change impacts on houses constructed in accordance with current Belgian legislation.

Highlights

- Multi-indicator evaluation is performed to assess overheating during short-term heatwaves
- Overheating in houses will be aggravated by the continuation of global warming
- Thermal comfort optimization does not ensure overheating prevention during extreme events

Introduction

Climate change caused by natural and anthropogenic sources is expected to increase the global surface temperature by 1-5.7℃ by the end of the century (IPCC WGII core writing team, 2022). The situation will be worse in the cities due to Urban Heat Island (UHI) effect, which typically are 5 ℃ -10 ℃ warmer compared to surrounding areas (Bohnenstengel et al., 2011; Oke, 1995). With the continuation of global warming, future heatwaves are predicted to become more severe and prolonged (Brown, 2020; Witze, 2022). Heatwaves, a period of sweltering weather (McGregor, 2015), can lead to overheating problems in houses, causing serious issues for the occupants (Hooyberghs et al., 2017; Lan et al., 2017). During the hot summer of 2003, more than 2500 excess deaths were reported across Europe (Climate Centre, 2020), highlighting the urgency to enhance the thermal performance of houses to keep occupants safe during hot weather conditions.

Many studies attempted to evaluate thermal comfort in houses during heatwaves. Ozarisoy (2022) analyzed thermal comfort conditions in a terraced house in Watford, UK, and found that indoor temperatures remained high during heatwaves, especially in the first-floor bedrooms. Laouadi et al. (2020) evaluated overheating risk in a typical detached house in Ontario, Canada, and found that naturally ventilated houses were unable to fully satisfy the overheating criteria during heatwaves. Zhou et al. (2020) analyzed overheating risk in a residential unit in Zurich, Switzerland, and found that different room orientations resulted in varying levels of overheating. Kwok et al. (2017) examined four types of Public Rental Housing (PRC) in Hong Kong and found that overheating occurred in all cases but with different durations and intensities.

So far, few studies have evaluated current and future overheating conditions using a multi-indicator approach (coupling heat stress and comfort indices) during concurrent heatwaves and the cooling system outage. This study is developed as part of the International Energy Agency (IEA) EBC Annex 80 project to address the abovementioned knowledge gap. The study aims to expand knowledge on evaluating overheating risks in high-performance houses during critical conditions in the context of climate change.

Methodology

This section provides the methodology implemented for the current study based on the simulation-based framework developed by (Rahif, Hamdy, et al., 2022). Initially, three Optimal Solutions (OSs) are adopted from (Rahif et al., 2023), in which the original house model is optimized using 13 passive design strategies to improve thermal comfort and HVAC energy performance using Genetic Algorithm (GA) based on Non-dominated Sorting Genetic Algorithm 2 (NSGA-II) method. As shown in Figure 1, the three cases from the Pareto front include the most thermally comfortable solution, OS01, which is also the solution with the highest final energy use for HVAC. On the other hand, the optimal solution for energy efficiency, OS02, has the highest discomfort. The compromise solution, OS03, is to balance energy efficiency and thermal comfort. The ranges/options of the passive design strategies as the input factors for optimization and the characteristics of the optimal solutions are listed in Table 1. Subsequently, simulations are conducted assuming that the cooling system was out of service during short-term heatwaves for the chosen optimal solutions.

https://doi.org/10.26868/25222708.2023.1195

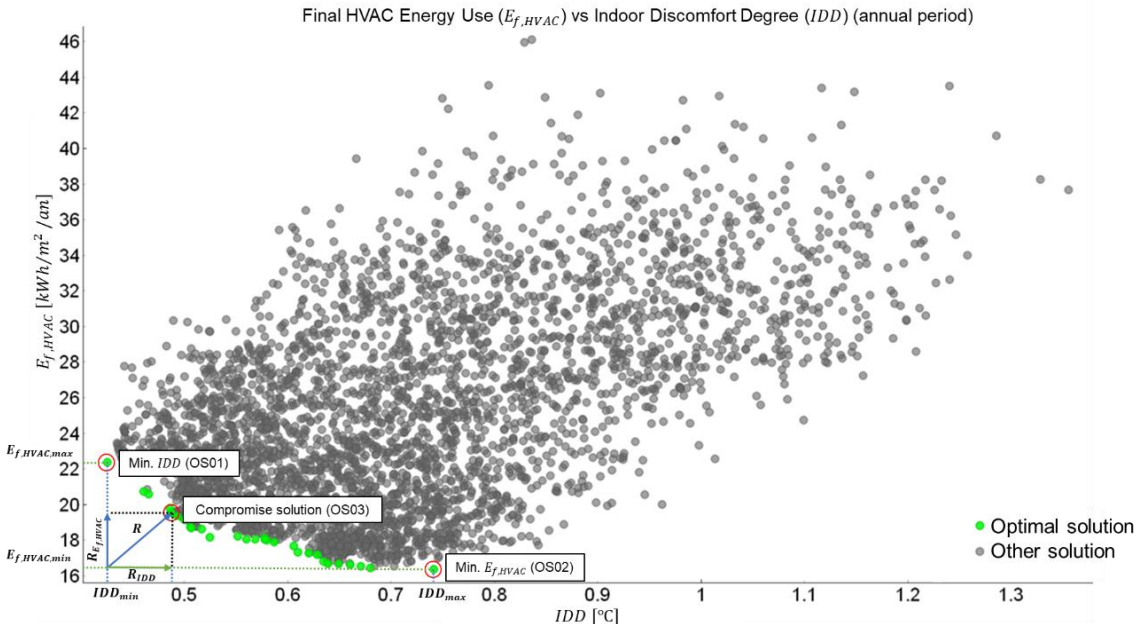

Figure 1. A scatter plot to display the relationship between the final energy use of HVAC ($E_{f,HVAC}$) and Indoor Discomfort Degree (IDD) for all optimization cases. The plot includes a green Pareto front and highlights three optimal solutions. Derived from (Rahif et al., 2023).

Table 1. The characteristics of the selected optimal solutions: minimum Indoor Discomfort Degree (IDD) case (OS01), minimum final HVAC energy use ($E_{f,HVAC}$) case (OS02), and compromise solution case (OS03). Derived from (Rahif et al., 2023).

Optimal solutions													
Min. *IDD* (OS01)	**Factors**												
	F1	F2	F3	F4	F5	F6	F7	F8	F9	F10	F11	F12	F13
	5	135	0.50	0.60	0.10	Roller blind	U0.8-SHGC0.8	UPVC	U0.1-ThM3000	U0.1-ThM2000	U1-ThM3000W	U1-ThM3000W	U0.1-ThM3000 + GR
Min. $E_{f,HVAC}$ (OS02)	**Factors**												
	F1	F2	F3	F4	F5	F6	F7	F8	F9	F10	F11	F12	F13
	5	315	0.40	0.40	0.10	Roller blind	U0.8-SHGC0.2	UPVC	U0.1-ThM3000	U0.1-ThM1000	U1-ThM3000W	U0.8-ThM3000	U0.1-ThM2000 + GR
Compromise solution (OS03)	**Factors**												
	F1	F2	F3	F4	F5	F6	F7	F8	F9	F10	F11	F12	F13
	5	135	0.80	0.50	0.10	Roller blind	U0.8-SHGC0.5	Painted wood	U0.1-ThM3000	U0.1-ThM1000	U1-ThM3000W	U1 - ThM3000	U0.1-ThM3000 + GR

Ranges/options of input factors → F1: Natural ventilation rate (Min=1, Max=5, Step=2) [ac/h], F2: Buidling orientation (Min=135, Max=315, Step=180) [°], F3: Wall solar absorptance (Min=0.40, Max=0.90, Step=0.10) [-], F4: Roof solar absorptance (Min=0.40, Max=0.80, Step=0.10) [-], F5: Infiltration rate (Min=0.10, Max=1.20, Step=0.10) [ac/h], F6: Shading strategy [no shading, electrochromic glazing, roller blind, venetian blind], F7: Glazing type (Thermochromic, U0.8-SHGC0.2, U0.8-SHGC0.5, U0.8-SHGC0.8, U0.9-SHGC0.2, U0.9-SHGC0.5, U0.9-SHGC0.8, U1-SHGC0.2, U1-SHGC0.5, U1-SHGC0.8, U1.1-SHGC0.2, U1.1-SHGC0.5, U1.1-SHGC0.8, U1.2-SHGC0.2, U1.2-SHGC0.5, U1.2-SHGC0.8), F8: Widnow frame type (Aluminum frame with no thermal break, Aluminum frame with thermal break, Painted wood, UPVC), F9: External wall construction (U0.1-ThM1000, U0.1-ThM2000, U0.1-ThM3000, U0.2-ThM1000, U0.2-ThM2000, U0.2-ThM3000, U0.3-ThM1000, U0.3-ThM2000, U0.3-ThM3000), F10: Ground floor construction (U0.1-ThM1000, U0.1-ThM2000, U0.1-ThM3000, U0.2-ThM1000, U0.2-ThM2000, U0.2-ThM3000, U0.3-ThM1000, U0.3-ThM2000, U0.3-ThM3000), F11: Internal wall construction (U1-ThM1000, U1-ThM2000, U1-ThM3000, U1.5-ThM1000, U1.5-ThM2000, U1.5-ThM3000, U2-ThM1000, U2-ThM2000, U2-ThM3000), F12: Internal floor construction (U0.8-ThM1000, U0.8-ThM2000, U0.8-ThM3000, U0.9-ThM1000, U0.9-ThM2000, U0.9-ThM3000, U1-ThM1000, U1-ThM2000, U1-ThM3000), F13: Roof construction (U0.1-ThM1000, U0.1-ThM1000+GR*, U0.1-ThM2000, U0.1-ThM2000+GR, U0.1-ThM3000, U0.1-ThM3000+GR, U0.2-ThM1000, U0.2-ThM1000+GR, U0.2-ThM2000, U0.2-ThM2000+GR, U0.2-ThM3000, U0.2-ThM3000+GR, U0.3-ThM1000, U0.3-ThM1000+GR, U0.3-ThM2000, U0.3-ThM2000+GR, U0.3-ThM3000, U0.3-ThM3000+GR). * Green Roof → substrate layer = 15 cm, drainage layer = 5 cm, plant height = 0.1 m, leaf reflectivity = 0.22, and leaf emissivity = 0.95 (Kazemi et al., 2023; Kazemi & Courard, 2021; Norouziasas et al., 2023).

DesignBuilder v7.0.0, a Graphical User Interface (GUI) for the EnergyPlus simulation engine, is used to conduct the simulations. Microsoft Excel and an in-house open-source MATLAB script are used for post-processing and visualization of the results (Rahif & Attia, 2022) (https://doi.org/10.5281/zenodo.7326901).

Boundary conditions

The boundary conditions of this study are described below:

1. The research is carried out on a case study situated in a temperate oceanic climate (Cfb). Such regions are heating-dominated, resulting in building designs focused on heat retention to minimize energy consumption for heating. Consequently, there is a higher possibility of overheating during the summer months (McLeod & Swainson, 2017).
2. A particular building typology was chosen as the representative example, which is a single-family nearly Zero-Energy terraced dwelling. These houses are prone to overheating due to their high insulation and airtightness requirements (Mitchell & Natarajan, 2019). Provisions are required to extend the findings to other building typologies (Attia et al., 2020).

House model

This paper selects a representative case of a three-story terraced dwelling located in Woluwe-Saint-Lambert municipality in Brussels based on the work of (Attia et al., 2022) (see Figure 2). The simulation model used in this paper is adopted from (Attia, 2021), which has been validated using public statistics and utility bills between 2015-2019.

The house is occupied by a family of four and was originally heated by a gas-fired boiler and mechanically/naturally ventilated. The boiler was replaced with a reversible air-to-water heat pump for heating and cooling, along with mechanical/natural ventilation, based on previous research (Rahif, Norouziasas, et al., 2022; Zhang et al., 2021). The HVAC components' capacities and design flow rates are auto-sized using the ASHRAE sizing method (ANSI/ASHRAE Handbook, 2017). More detailed information on the house and HVAC characteristics can be found in (Attia et al., 2022; Rahif, Norouziasas, et al., 2022) and (Rahif et al., 2023).

Climate data

In studies related to climate change, obtaining high-quality weather data is crucial. This research employs weather data derived from General Circulation Models (GCMs), which are transformed using a dynamical downscaling technique called Regional Climate Model (MAR). Two methods were used to generate the weather data: MAR ERA5, which is based on observed climate data, and MAR BCC-CSM2-MR based on the projected climate scenario under the most plausible emission trajectory SSP2-4.5 (Pielke Jr et al., 2022). MAR BCC-CSM2-MR was validated using the results of MAR ERA5 to confirm whether it can be used to calculate future climate data.

Based on the climate data derived from MAR, the heatwaves were detected during three different periods: 2001-2020, 2041-2060, and 2080-2100. For this aim, the static heatwave definition by the Royal Meteorological Institute (RMI) of Belgium (i.e., a period of at least five consecutive days with a maximum air temperature higher than 25℃, in which at least three days have a maximum air temperature higher than 30℃) is coupled to a statistical method by (Ouzeau et al., 2016). The identified heatwaves were characterized by their duration, intensity, and maximal temperature. This paper selects the highest maximal temperature heatwave for each period, which was detected in 2019 during 2001-2020, in 2047 during 2041-2060, and 2098 during 2081-2100. It should be mentioned that the choice of time periods in this study is based on the suggestions from the guidelines presented by the International Energy Agency (IEA) EBC Annex 80 project (Attia et al., 2021; Zhang et al., 2023). All weather data are obtained from (Doutreloup et al., 2022).

Figure 2. The image showcases the south-facing façade and the DesignBuilder simulation model of a nearly Zero-Energy terraced dwelling in Belgium, which serves as a benchmark for sustainable house design (Rahif et al., 2023).

Thermal comfort models and indicators

Overheating assessments require the determination of thermal comfort models (if necessary) and indices.

Thermal comfort models can be divided into major groups: static and adaptive. The static thermal comfort models establish fixed thresholds that identify when an environment becomes too hot, whereas the adaptive comfort models establish variable thresholds based on outdoor weather conditions. An important part of the adaptive model is human feedback, which may require some sensors such as heart rate monitors, eye movement meters, skin temperature sensors, etc. The questionnaires often used are also complementary tool. This study employs both models, using the category-based thresholds outlined in ISO 17772-1, including Cat. I, Cat. II, Cat. III, and Cat. IV (only for static model). In this paper, Cat. II is selected, which is recommended for new buildings and refurbishments. For the static model, ISO 17772-1 provides thresholds in terms of operative temperature, which are translated from the *PMV/PPD*

https://doi.org/10.26868/25222708.2023.1195

limits under certain assumptions. The maximum threshold for Cat. II is set at 26℃. For the adaptive model, ISO 17772-1 provides equations based on the running mean outdoor air temperature T_{rmo} [℃]. The formula to calculate the maximum threshold for Cat. II is,

$$0.33T_{rmo} + 18.8 + 3 \quad (1)$$
$$where\ 10℃ < T_{rmo} < 30℃$$

Previous studies have explored various metrics for measuring overheating in buildings, as documented by (Attia et al., 2023; Carlucci & Pagliano, 2012; Enescu, 2017; Rahif et al., 2021). In this study, the authors choose to focus on three metrics - Heat Index (HI), Thermal Autonomy (TA), and Indoor Overheating Degree (IOhD) - to evaluate the thermal performance of the building in a more composite, complex, and informative way. The *HI* [℃] metric combines relative humidity and air temperature to quantify how hot the human body feels. This metric has resulted from multiple regression analyses by (Rothfusz & Headquarters, 1990) and requires adjustments for different ranges of air temperature (T_{air}) and relative humidity (RH). It is proposed by (RELi 2.0., 2020) to ensure thermal safety during power outages. The *HI* metric is being widely used in environmental health research and recent studies (Rempel et al., 2022; Sun et al., 2020; Zune et al., 2020). The formula to calculate *HI* is,

$$\begin{aligned} HI = &-42.379 + 2.04901523 \times T_{air} \quad (2)\\ &+ 10.1333127 \times RH\\ &- 0.22475541 \times T_{air} \times RH\\ &- 0.00683783 \times T_{air}^2\\ &- 0.05481717 \times RH^2\\ &+ 0.00122874 \times T_{air}^2 \times RH\\ &+ 0.00085282 \times T_{air} \times RH^2\\ &- 0.00000199 \times T_{air}^2 \times RH^2 \end{aligned}$$

Where *SQRT* and *ABS* are square root function and absolute value, respectively. The *TA* [%] metric measures the percentage of time when the building's thermal zone meets the specified comfort criteria, only relying on passive measures (Levitt et al., 2013). The *TA* is particularly relevant for assessing the building's thermal performance during a power outage when the active cooling system is not operable (assuming no backup power). The formula to calculate the *TA* is,

$$TA = \frac{\sum_{i=1}^{occupied\ hours} wf_i}{\sum_{i=1}^{occupied\ hours} h_i} \quad (3)$$
$$where \begin{cases} wf_i = 1\ ;\ T_{in} < T_{comfort,upper} \\ wf_i = 0\ ;\ T_{in} > T_{comfort,upper} \end{cases}$$

The *IOhD* [℃] is a multizonal metric that is asymmetric and accumulates cooling degree hours over the total number of hours the zones are occupied (Hamdy et al., 2017). The formula used to calculate *IOhD* is,

$$IOhD \equiv \frac{\sum_{z=1}^{Z}\sum_{i=1}^{N_{occ}(z)}\left[\left(T_{in,z,i} - T_{comf,upper,z,i}\right)^{+} \times h_{i,z}\right]}{\sum_{z=1}^{Z}\sum_{i=1}^{N_{occ}(z)} t_{i,z}} \quad (4)$$

Where Z [-] is the total number of building zones, z is zone counter, $N_{occ}(z)$ [-] is the total number of occupied hours in zone z, i is hour counter, $T_{in,o,z}$ [℃] is the indoor operative temperature in zone z at hour i, $T_{comf,upper,z,i}$ [℃] is maximum comfort threshold in zone z at hour i, $T_{comf,lower,z,i}$ [℃] is the minimum comfort threshold in zone z at hour i.

Results

Current and future heatwaves

Figure 3 illustrates the outdoor dry-bulb temperature during the three most extreme heatwaves from 2001-2020, 2041-2060, and 2081-2100 and Table 2 summarizes their main characteristics. Typically, these heatwaves begin towards the end of June and end no later than early July. The findings demonstrate that future heatwaves will be more severe and extended in duration. Specifically, the heatwave that occurred in 2019 lasted for five days, while those in 2047 and 2098 persisted for seven and ten days, respectively. In terms of mean air temperature, there is a rise of 3.28% in 2047 and 12.15% in 2098 in comparison to the mean air temperature obtained in 2019.

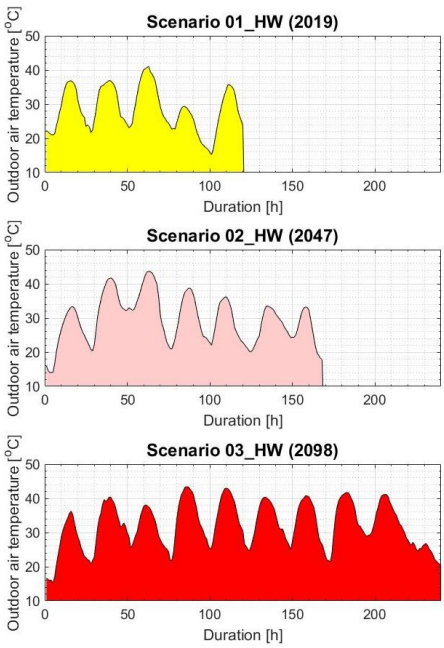

Figure 3. Visualizing hourly outdoor air temperature during the highest maximal temperature heatwaves in the coming decades: 2001-2020 (in 2019), 2041-2060 (in 2047), and 2081-2100 (in 2098) (Rahif et al., 2023).

Table 2. Overview of key characteristics of the three heatwave scenarios.

	Scenario 01_HW (2019)	**Scenario 02_HW (2047)**	**Scenario 03_HW (2098)**
Date	25 Jun-29 Jun	25 Jun-01 Jul	26 Jun-05 Jul
Duration [days]	5	7	10
Max. Air Temperature [℃]	41.02	43.64	43.37
Avg. Air Temperature [℃]	28.64	29.58	32.12

https://doi.org/10.26868/25222708.2023.1195

Overheating during heatwaves

Table 3 presents a summary of the zonal maximum operative temperature, maximum Heat Index (HI), and Thermal Autonomy (TA) for three optimal solutions (OS01, OS02, and OS03). As mentioned earlier, it is assumed that the cooling system is not operating during the heatwaves, and the house relies only on passive measures. The results show that during the heatwaves, except OS02, other cases exceeded the recommended healthy limit of 32 ℃ according to World Health Organization (WHO). In the most critical zone, bedroom 02, the maximum operative temperature in OS01 reached 32.86 ℃ during the 2019 heatwave and increased to 34.53 ℃ in 2098. Meanwhile, in OS02, the maximum operative temperature in the most critical zone, the workspace, was 28.09 ℃ during the 2019 heatwave and increased to 29.35 ℃ in 2098. In OS03, the maximum operative temperature in bedroom 02 reached 31.27 ℃ during the 2019 heatwave and increased to 33.64 ℃ in 2098. Moreover, all bedroom temperatures exceeded the healthy sleeping temperature limit of 24℃ recommended by WHO.

RELi 2.0 recommends that the *HI* in residential units should not exceed 32.2℃ during hot seasons. The study found that OS01 and OS03 were unable to maintain this limit for Bedroom 02 in all three heatwave scenarios, putting occupants at risk of heat-related illnesses. However, OS02 was successful in keeping the HI below the recommended limit in all scenarios.

Overall, climate change causes a reduction in *TA* by 17% to 28% during heatwaves in selected optimal solutions. When using the static comfort model, OS01 has an average *TA* value of 32.67%, OS02 has an average *TA* value of 73.35%, and OS03 has an average *TA* value of 46.98%. When using the adaptive comfort model, OS01 has an average *TA* value of 31.62%, OS02 has an average *TA* value of 80.94%, and OS03 has an average *TA* value of 49.07%. According to Table 3, shifting from a static comfort model to an adaptive one usually leads to higher *TA* values. However, this may not always be the case, as the maximum temperature limit in the adaptive comfort model can decrease to 25℃ in Category II (which is 1℃ lower than the static threshold of 26℃). This means that if the indoor temperature fluctuates between 25℃-26℃, it will be considered autonomous based on the static comfort model but not according to the adaptive model. This is particularly noticeable in current climatic conditions, where lower running mean outdoor temperatures are observed. While this may be valid for temperate regions like Brussels, it might not be applicable to warmer climates (Piderit et al., 2019).

Figure 4 shows that OS01 has the highest *IOhD* value of 1.84℃ in the 2098 heatwave scenario, which suggests that the house configuration used in OS01 has the highest risk of overheating in the future. Additionally, the study observed that as heatwave events worsen in the future, the difference in *IOhD* between the optimal cases (i.e., OS01, OS02, and OS03) increases. For example, in the 2019 heatwave, the *IOhD* difference between OS01 and OS02 is 0.87℃, whereas, in the 2098 heatwave, it increases to 1.57℃. This implies that the house configuration used in OS02 and OS03 is more effective in reducing the risk of overheating in future heatwave scenarios compared to OS01. It is also found that switching from a static comfort model to an adaptive one leads to a decrease in the *IOhD* by 12% in OS01, by 47% in OS02, and by 20% in OS03 averaged over all heatwave scenarios.

Conclusion

Climate change has increased in the past century and will continue to increase the average global temperature, leading to more severe heatwaves. Multiple effective passive strategies have been developed so far that can limit the health, productivity, and well-being impacts of overheating during heatwaves. By comparing the optimal solutions, for the case of a nearly zero-energy terraced dwelling in a temperate region, high ventilation rates, low infiltration rates, high insulation levels, high thermal mass, integration of green roofs, and operable roller blinds contribute to energy efficiency and thermal comfort. However, with the continuation of global warming, passive cooling strategies in buildings will become less effective (Mahar et al., 2020), and power supply failures will be more common due to the heavy use of air conditioning. This study shows that none of the optimal solutions can fully suppress overheating during concurrent heatwaves and cooling system outages, which can cause serious health issues for occupants. In total, four metrics are used to evaluate overheating/thermal comfort during short-term heatwaves. Those metrics are complementary and demonstrate the same result, which is the exacerbation of overheating with the continuation of global warming. Each of these metrics provides a unique perspective on the thermal performance of the house. For example, the *HI* metric focuses on the heat stress imposed on the occupants, the *TA* focuses on the ability of the house to passively survive during unprecedented events, and the *IOhD* shows the integrated overheating risk across different zones. Each of these metrics provides valuable insights, and when combined, they paint a complete picture of how the house is performing. This study emphasizes the need for governments and policymakers to promote proactive adaptation and establish clear targets for building stock to mitigate the overheating impact of climate change.

https://doi.org/10.26868/25222708.2023.1195

Table 3. The table summarizes the maximum operative temperature, maximum Heat Index (HI), and Thermal Autonomy (TA) based on static and adaptive thermal comfort models for various zones during three different heatwave scenarios: Scenario 01 HW (2019), Scenario 02 HW (2047), and Scenario 03 (2098).

OS01				
Scenario 01_HW (2019)				
Zone	Workspace	Living+kitchen	Bedroom 01	Bedroom 02
Max. Op. temperature [°C]	28.19	30.26	28.18	32.86
Max. Heat Index (HI) [°C]	29.29	31.35	29.19	33.61
Thermal autonomy (TA) S/A* [%]	36.36/37.31	23.10/13.63	65.15/63.63	24.62/16.14
Scenario 02_HW (2047)				
Max. Op. temperature [°C]	29.61	31.75	29.25	34.53
Max. Heat Index (HI) [°C]	29.60	31.31	29.05	33.60
Thermal autonomy (TA) S/A [%]	31.73/36.71	26.28/24.03	48.07/53.52	24.67/17.62
Scenario 03_HW (2098)				
Max. Op. temperature [°C]	30.06	33.31	29.83	35.61
Max. Heat Index (HI) [°C]	29.59	32.21	29.20	34.43
Thermal autonomy (TA) S/A [%]	31.71/30.44	23.43/20.83	38.80/50.26	20.31/15.53
OS02				
Scenario 01_HW (2019)				
Max. Op. temperature [°C]	28.09	27.03	27.19	26.68
Max. Heat Index (HI) [°C]	29.54	27.94	28.33	27.77
Thermal autonomy (TA) S/A [%]	73.10/76.3	84.47/84.09	85.60/87.75	91.66/91.67
Scenario 02_HW (2047)				
Max. Op. temperature [°C]	28.94	27.38	27.72	27.35
Max. Heat Index (HI) [°C]	29.37	28.05	27.97	27.71
Thermal autonomy (TA) S/A [%]	60.89/68.26	73.07/82.05	78.84/82.57	80.12/88.28
Scenario 03_HW (2098)				
Max. Op. temperature [°C]	29.35	28.80	28.27	27.95
Max. Heat Index (HI) [°C]	29.19	29.24	28.36	28.63
Thermal autonomy (TA) S/A [%]	62.76/71.97	63.80/79.42	75/77.88	75/81.09
OS03				
Scenario 01_HW (2019)				
Max. Op. temperature [°C]	27.36	29.63	28.48	31.27
Max. Heat Index (HI) [°C]	28.63	30.99	28.67	32.34
Thermal autonomy (TA) S/A [%]	71.59/67.18	31.81/27.34	84.47/83.33	40.53/37.87
Scenario 02_HW (2047)				
Max. Op. temperature [°C]	28.49	30.85	28.30	32.68
Max. Heat Index (HI) [°C]	28.84	30.80	28.39	32.29
Thermal autonomy (TA) S/A [%]	46.79/62.5	28.48/26.6	68.91/73.68	28.52/31.41
Scenario 03_HW (2098)				
Max. Op. temperature [°C]	28.91	32.23	28.83	33.64
Max. Heat Index (HI) [°C]	28.70	31.36	28.90	32.80
Thermal autonomy (TA) S/A [%]	46.61/57.69	26.04/24.24	65.36/71.79	24.74/25.26

*__(S)__ Static & __(A)__ Adaptive

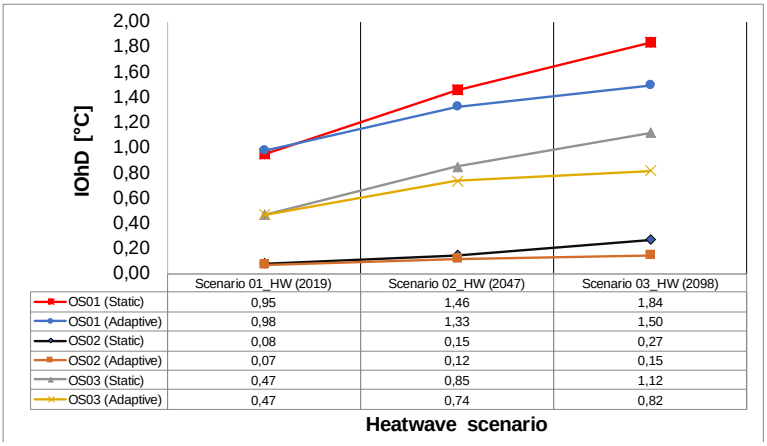

Figure 4. Indoor Overheating Degree (IOhD) presented by heatwave scenario based on static and adaptive thermal comfort models.

https://doi.org/10.26868/25222708.2023.1195

Acknowledgment

This research was funded by the Walloon Region under the call 'Actions de Recherche Concertées 2019 (ARC)' (funding number: ARC 19/23-05) and the project OCCuPANt, on the Impacts Of Climate Change on the indoor environmental and energy PerformAnce of buildiNgs in Belgium during summer. The authors would like to gratefully acknowledge the Walloon Region and the University of Liege for funding. We would like to also acknowledge the Sustainable Building Design (SBD) lab at the Faculty of Applied Sciences at the University of Liege for the use of 64-processor workstation during the computation. This work also has been written in collaboration with the Research Center on Zero Emission Neighbourhoods in Smart Cities (FME ZEN). The authors gratefully acknowledge the support of ZEN partners, Norway and the Research Council of Norway. This study is a part of the International Energy Agency (IEA) EBC Annex 80 – "Resilient cooling of buildings" project activities to define resilient cooling in residential buildings. No potential competing interest was reported by the authors.

References

ANSI/ASHRAE Handbook. (2017). *Handbook–2017: Fundamentals*.

Attia, S. (2021). Benchmark model for nearly-zero-energy terraced dwellings. *Harvard Dataverse, Cambridge, United States*. https://doi.org/10.7910/DVN/GJI84W

Attia, S., Benzidane, C., Rahif, R., Amaripadath, D., Hamdy, M., Holzer, P., Koch, A., Maas, A., Moosberger, S., Petersen, S., Mavrogianni, A., Maria Hidalgo-Betanzos, J., Almeida, M., Akander, J., Khosravi Bakhtiari, H., Kinnane, O., Kosonen, R., & Carlucci, S. (2023). Overheating calculation methods, criteria, and indicators in European regulation for residential buildings. *Energy and Buildings*, *292*, 113170. https://doi.org/10.1016/j.enbuild.2023.113170

Attia, S., Canonge, T., Popineau, M., & Cuchet, M. (2022). Developing a benchmark model for renovated, nearly zero-energy, terraced dwellings. *Applied Energy*, *306*, 118128. https://doi.org/10.1016/j.apenergy.2021.118128

Attia, S., Levinson, R., Ndongo, E., Holzer, P., Berk Kazanci, O., Homaei, S., Zhang, C., Olesen, B. W., Qi, D., Hamdy, M., & Heiselberg, P. (2021). Resilient cooling of buildings to protect against heat waves and power outages: Key concepts and definition. *Energy and Buildings*, *239*, 110869. https://doi.org/10.1016/j.enbuild.2021.110869

Attia, S., Shadmanfar, N., & Ricci, F. (2020). Developing two benchmark models for nearly zero energy schools. *Applied Energy*, *263*, 114614. https://doi.org/10.1016/j.apenergy.2020.114614

Bohnenstengel, S. I., Evans, S., Clark, P. A., & Belcher, S. E. (2011). Simulations of the London urban heat island. *Quarterly Journal of the Royal Meteorological Society*, *137*(659), 1625–1640. https://doi.org/10.1002/qj.855

Brown, S. J. (2020). Future changes in heatwave severity, duration and frequency due to climate change for the most populous cities. *Weather and Climate Extremes*, *30*, 100278. https://doi.org/10.1016/j.wace.2020.100278

Carlucci, S., & Pagliano, L. (2012). A review of indices for the long-term evaluation of the general thermal comfort conditions in buildings. *Energy and Buildings*, *53*, 194–205. https://doi.org/10.1016/j.enbuild.2012.06.015

Climate Centre. (2020, May 5). *European summer heatwaves the most lethal disaster of 2019, says international research group*. https://www.climatecentre.org/565/european-summer-heatwaves-the-most-lethal-disaster-of-2019-says-international-research-group/

Doutreloup, S., Fettweis, X., Rahif, R., Elnagar, E., Pourkiaei, M. S., Amaripadath, D., & Attia, S. (2022). Historical and future weather data for dynamic building simulations in Belgium using the regional climate model MAR: typical and extreme meteorological year and heatwaves. *Earth System Science Data*, *14*(7), 3039–3051. https://doi.org/10.5194/essd-14-3039-2022

Enescu, D. (2017). A review of thermal comfort models and indicators for indoor environments. *Renewable and Sustainable Energy Reviews*, *79*, 1353–1379. https://doi.org/10.1016/j.rser.2017.05.175

Hamdy, M., Carlucci, S., Hoes, P.-J., & Hensen, J. L. M. (2017). The impact of climate change on the overheating risk in dwellings—A Dutch case study. *Building and Environment*, *122*, 307–323. https://doi.org/10.1016/j.buildenv.2017.06.031

Hooyberghs, H., Verbeke, S., Lauwaet, D., Costa, H., Floater, G., & De Ridder, K. (2017). Influence of climate change on summer cooling costs and heat stress in urban office buildings. *Climatic Change*, *144*(4), 721–735. https://doi.org/10.1007/s10584-017-2058-1

IPCC WGII core writing team. (2022). *Summary for Policymakers: Climate Change 2022—Impacts, Adaptation, and Vulnerability*. (p. 7). p.7, IPCC Geneva, Switzerland. https://www.ipcc.ch/report/ar6/wg2/downloads/report/IPCC_AR6_WGII_FinalDraft_FullReport.pdf

Kazemi, M., & Courard, L. (2021). Modelling hygrothermal conditions of unsaturated substrate and drainage layers for the thermal resistance assessment of green roof: Effect of coarse recycled materials. *Energy and Buildings*, *250*, 111315. https://doi.org/10.1016/j.enbuild.2021.111315

Kazemi, M., Rahif, R., Courard, L., & Attia, S. (2023). Sensitivity analysis and weather condition effects on hygrothermal performance of green roof models characterized by recycled and artificial materials' properties. *Building and Environment*, *237*, 110327. https://doi.org/10.1016/j.buildenv.2023.110327

Kwok, Y. T., Lai, A. K. L., Lau, K. K.-L., Chan, P. W., Lavafpour, Y., Ho, J. C. K., & Ng, E. Y. Y. (2017). Thermal comfort and energy performance of public rental housing under typical and near-extreme weather conditions in Hong Kong. *Energy and Buildings*, *156*, 390–403. https://doi.org/10.1016/j.enbuild.2017.09.067

Lan, L., Tsuzuki, K., Liu, Y., & Lian, Z. (2017). Thermal environment and sleep quality: A review. *Energy and Buildings*, *149*, 101–113. https://doi.org/10.1016/j.enbuild.2017.05.043Get

Laouadi, A., Bartko, M., & Lacasse, M. A. (2020). A new methodology of evaluation of overheating in buildings. *Energy and Buildings*, *226*, 110360. https://doi.org/10.1016/j.enbuild.2020.110360

Levitt, B., Ubbelohde, M., Loisos, G., & Brown, N. (2013). *Thermal autonomy as metric and design process*. 47–58.

Mahar, W. A., Verbeeck, G., Reiter, S., & Attia, S. (2020). Sensitivity analysis of passive design strategies for residential buildings in cold semi-arid climates. *Sustainability*, *12*(3), 1091. https://doi.org/10.3390/su12031091

McGregor, G. (2015). *Heatwaves and health: Guidance on warning-system development*. World Meterorological Organisation; World Health Organisation. https://www.who.int/globalchange/publications/heatwaves-health-guidance/en/

McLeod, R. S., & Swainson, M. (2017). Chronic overheating in low carbon urban developments in a temperate climate. *Renewable and Sustainable Energy Reviews*, *74*, 201–220. https://doi.org/10.1016/j.rser.2016.09.106

Mitchell, R., & Natarajan, S. (2019). Overheating risk in Passivhaus dwellings. *Building Services Engineering Research and Technology*, *40*(4), 446–469. https://doi.org/10.1177/0143624419842000

Norouziasas, A., Tabadkani, A., Rahif, R., Amer, M., van Dijk, D., Lamy, H., & Attia, S. (2023). Implementation of ISO/DIS 52016-3 for adaptive façades: A case study of an office building. *Building and Environment*, *235*, 110195. https://doi.org/10.1016/j.buildenv.2023.110195

Oke, T. (1995). The heat island of the urban boundary layer: Characteristics, causes and effects. *Wind Climate in Cities*, 81–107. https://doi.org/10.1007/978-94-017-3686-2_5

Ouzeau, G., Soubeyroux, J.-M., Schneider, M., Vautard, R., & Planton, S. (2016). Heat waves analysis over France in present and future climate: Application of a new method on the EURO-CORDEX ensemble. *Climate Services*, *4*, 1–12. https://doi.org/10.1016/j.cliser.2016.09.002

Ozarisoy, B. (2022). Energy effectiveness of passive cooling design strategies to reduce the impact of long-term heatwaves on occupants' thermal comfort in Europe: Climate change and mitigation. *Journal of Cleaner Production*, *330*, 129675. https://doi.org/10.1016/j.jclepro.2021.129675

Piderit, M. B., Vivanco, F., Van Moeseke, G., & Attia, S. (2019). Net zero buildings—A framework for an integrated policy in Chile. *Sustainability*, *11*(5), 1494. https://doi.org/10.3390/su11051494

Pielke Jr, R., Burgess, M. G., & Ritchie, J. (2022). Plausible 2005–2050 emissions scenarios project between 2° C and 3° C of warming by 2100. *Environmental Research Letters*, *17*(2), 024027. https://doi.org/10.1088/1748-9326/ac4ebf

Rahif, R., Amaripadath, D., & Attia, S. (2021). Review on Time-Integrated Overheating Evaluation Methods for Residential Buildings in Temperate Climates of Europe. *Energy and Buildings*, *252*, 111463. https://doi.org/10.1016/j.enbuild.2021.111463

Rahif, R., & Attia, S. (2022). IOhD (Calculation & illustration), IOcD (Calculation & illustration), AWD (Calculation & illustration), ACD (Calculation & illustration), CCOhR (Calculation), CCOcR (Calculation), Zonal OpT (illustration), and HWs (illustration) v01. *Zenodo*. https://doi.org/10.5281/zenodo.7326901

Rahif, R., Hamdy, M., Homaei, S., Zhang, C., Holzer, P., & Attia, S. (2022). Simulation-based framework to evaluate resistivity of cooling strategies in buildings against overheating impact of climate change. *Building and Environment*, 108599. https://doi.org/10.1016/j.buildenv.2021.108599

Rahif, R., Kazemi, M., & Attia, S. (2023). Overheating Analysis of Optimized Nearly Zero-Energy Dwelling During Current and Future Heatwaves Coincided with Cooling System Outage. *Energy and Buildings, In Press.*

Rahif, R., Norouziasas, A., Elnagar, E., Doutreloup, S., Pourkiaei, S. M., Amaripadath, D., Romain, A.-C., Fettweis, X., & Attia, S. (2022). Impact of climate change on nearly zero-energy dwelling in temperate climate: Time-integrated discomfort, HVAC energy performance, and GHG emissions. *Building and Environment*, *223*, 109397. https://doi.org/10.1016/j.buildenv.2022.109397

RELi 2.0. (2020). *Rating Guidelines for Resilient Design + Construction*. U.S. Green Building Council.

Rempel, A. R., Danis, J., Rempel, A. W., Fowler, M., & Mishra, S. (2022). Improving the passive survivability of residential buildings during extreme heat events in the Pacific Northwest. *Applied Energy*, *321*, 119323. https://doi.org/10.1016/j.apenergy.2022.119323

Rothfusz, L. P., & Headquarters, N. S. R. (1990). The heat index equation (or, more than you ever wanted to know about heat index). *Fort Worth, Texas: National Oceanic and Atmospheric Administration, National Weather Service, Office of Meteorology*, *9023*.

Sun, K., Specian, M., & Hong, T. (2020). Nexus of thermal resilience and energy efficiency in buildings: A case study of a nursing home. *Building and Environment*, *177*, 106842. https://doi.org/10.1016/j.buildenv.2020.106842

Witze, A. (2022). Extreme heatwaves: Surprising lessons from the record warmth. *Nature*, *608*(7923), 464–465. https://doi.org/10.1038/d41586-022-02114-y

Zhang, C., Kazanci, O. B., Attia, S., Levinson, R., Lee, S. H., Holzer, P., Rahif, R., Salvati, A., Machard, A., Pourabdollahtootkaboni, M., Gauri, A., Olesen, B. W., & Heiselberg, P. K. (2023). *IEA EBC Annex 80—Dynamic simulation guideline for the performance testing of resilient cooling strategies: Version 2* (DCE Technical Reports No. 306). Aaalborg University.

Zhang, C., Kazanci, O. B., Levinson, R., Heiselberg, P., Olesen, B. W., Chiesa, G., Sodagar, B., Ai, Z., Selkowitz, S., Zinzi, M., Mahdavi, A., Teufl, H., Kolokotroni, M., Salvati, A., Bozonnet, E., Chtioui, F., Salagnac, P., Rahif, R., Attia, S., … Zhang, G. (2021). Resilient cooling strategies – A critical review and qualitative assessment. *Energy and Buildings*, *251*, 111312. https://doi.org/10.1016/j.enbuild.2021.111312

Zhou, X., Carmeliet, J., Sulzer, M., & Derome, D. (2020). Energy-efficient mitigation measures for improving indoor thermal comfort during heat waves. *Applied Energy*, *278*, 115620. https://doi.org/10.1016/j.apenergy.2020.115620

Zune, M., Rodrigues, L., & Gillott, M. (2020). The vulnerability of homes to overheating in Myanmar today and in the future: A heat index analysis of measured and simulated data. *Energy and Buildings*, *223*, 110201. https://doi.org/10.1016/j.enbuild.2020.110201